JOURNAL OF SPACECRAFT AND ROCKETS
Vol. 31, No. 6, November–December 1994

Effect of a Baffle on Slosh Waves Excited by Gravity-Gradient Acceleration in Microgravity

R. J. Hung* and C. C. Lee†
University of Alabama in Huntsville, Huntsville, Alabama 35899

The dynamical behavior of fluids affected by an asymmetric gravity-gradient acceleration is studied. The effect of surface tension on rotating fluids, applicable to a partially filled full-scale Gravity Probe-B Spacecraft Dewar tank with and without installing baffle boards, is studied. Results of slosh-wave excitation along the liquid-vapor interface induced by gravity-gradient acceleration are examined. These results indicate that the gravity-gradient acceleration is equivalent to the combined effect of a twisting force and torsional moment acting on the spacecraft. The results are clearly seen from the eccentric contour of a bubble revolving around the axis of a Dewar in a horizontal r-θ plane. As the viscous force across the liquid-solid interface greatly contributes to the damping of slosh-wave excitation, installing baffles in the rotating Dewar is expected to dampen these waves. Results show that the damping effect provided by a baffle reduces the amplitude of slosh-wave excitation and lowers the degree of asymmetry in the liquid-vapor distribution. Computation of bubble (helium vapor) mass-center fluctuations also verifies that rotating a Dewar with baffles installed produces less fluctuation than without the baffles.

Nomenclature

$\hat{a}_{gg}$	= $(a_{gg,r}, a_{gg,\theta}, a_{gg,z})$, components of gravity-gradient vector in cylindrical coordinates
$\hat{d}$	= vector (not a unit vector) from the fluid element to the spacecraft mass center
g_0	= Earth gravity acceleration, 9.81 m/s^2
h	= spacecraft orbit altitude, 650 km for GP-B
L	= height of Dewar tank, cm
n	= orbit rate of spacecraft, 1.07×10^{-3} rad/s for GP-B
(r, θ, z)	= cylindrical coordinates
R_c	= radius of spacecraft circular orbit, $R_E + h = 7023$ km for GP-B
$\hat{r}_c$	= unit vector from the spacecraft mass center to the center of Earth
R_E	= radius of Earth, 6373 km
t	= time
(u, v, w)	= velocity components in cylindrical coordinates
μ	= viscous coefficient of fluid
ρ	= density of fluid
τ	= spacecraft gravity turnaround time, s
τ_0	= orbit period of spacecraft, 97.6 min for GP-B
ψ_E	= azimuth angle of Earth at the spacecraft mass center
ω	= angular velocity of spacecraft spinning about the z axis

Subscripts

L	= liquid
V	= vapor

Introduction

SOME experimental spacecraft use superconducting sensors for gyro readout and maintain a very low temperature for mechanical stability. The approaches to both cooling and control involve the use of superfluid liquid helium. For example, the Gravity Probe-B (GP-B) spacecraft uses the boiloff from the cryogenic liquid-helium Dewar as a propellant to maintain the attitude control and drag-free operation of the spacecraft.[1] Problems for attitude control (Fig. 1) may arise from asymmetry in the static liquid-helium distribution or to perturbations in the free surface. It may be required to install baffle boards inside the Dewar container (as shown in Fig. 1) so as to reduce the asymmetry in the liquid-vapor distribution.

For the GP-B spacecraft, cryogenic liquid helium II at a temperature of 1.8 K is used as the propellant. Because of its superfluidity, there are no temperature gradients in the liquid-helium. In the absence of temperature gradient along the surface to drive Marangoni convection, the equilibrium shape of the free surface is governed by a balance of capillary, centrifugal, and gravitational forces. In comparing the effects of surface tension with the effects of gravitational forces on the free surface of a liquid, it was found that the surface-tension force for most liquids is much greater than the gravitational force in a $10^{-8} g_0$ environment and lower. In other words, the equilibrium shape of the liquid-helium free surface in the operational GP-B Spacecraft is governed by a balance of capillary and centrifugal forces, and one may ignore the effect of gravitational force. Determination of vapor profiles based on computational experiments can uncover details of the flow that cannot be easily visualized or measured experimentally in a microgravity environment.

An instability of the liquid surface can be induced by the presence of longitudinal and lateral accelerations, vehicle vibration, and rotational fields of the spacecraft. Thus, slosh waves are excited, producing high- and low- frequency oscillations in the liquid propellant. The sources of the residual accelerations include the effects of the Earth's gravity gradient and atmospheric drag on the spacecraft, and spacecraft attitude motions arising from machinery vibrations, thruster firings, and crew motion. A recent study[2] suggests that high-frequency accelerations may be unimportant in comparison with the residual motions caused by low-frequency accelerations.

The time-dependent dynamical behavior of rotating fluids in reduced-gravity environments was simulated by numerically solving the Navier-Stokes equations subject to the initial and the boundary conditions.[3–5] At the interface between the liquid and the gaseous fluids, both the kinematic surface boundary condition and the interface stress conditions for components tangential and normal to the interface were applied.[3–5] The initial conditions were adopted from the steady-state formulations developed by Hung et al.[3] for the geometry of the GP-B spacecraft.[1] Some of the steady-state formulations of interface shapes were compared with the available experiments carried out by Leslie[6] in a free-falling aircraft (KC-135). The experiments carried out by Mason et al.[7] showed that the

Received March 15, 1993; revision received Dec. 27, 1993; accepted for publication March 10, 1994.

*Professor, Department of Mechanical and Aerospace Engineering. Associate Fellow AIAA.

†Senior Research Associate, Department of Mechanical and Aerospace Engineering. Member AIAA.

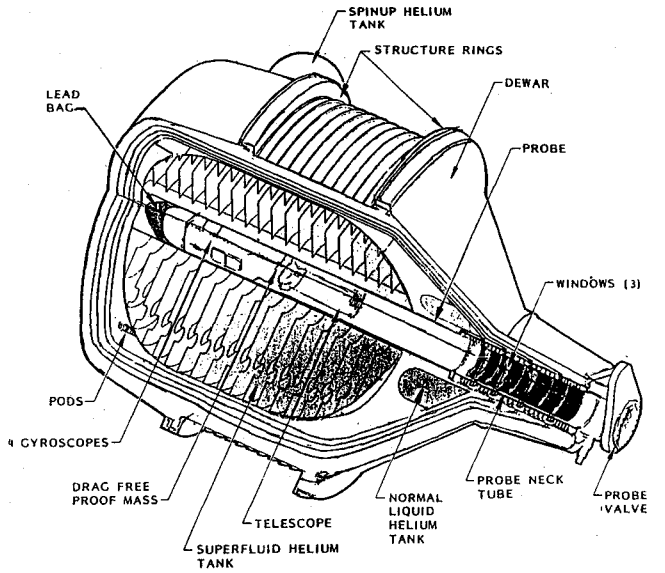

Fig. 1 GP-B module, showing the main elements of the liquid-helium Dewar, probe, and baffle boards.

classical fluid-mechanics theory is applicable for liquid helium in large containers.

The propellant tank will not be spinning in the GP-B spacecraft when it is deployed. In the early stages of the experiment, a spin rate of up to about 1 rpm will be imposed for instrument calibration. After calibration, the rotation rate will be reduced to its operational value of approximately 0.1 rpm.

In a spacecraft in orbit around the Earth, the azimuth angle of the Earth at the spacecraft mass center varies from 0 (along the axis of rotation) to 360 deg.

As the spacecraft moves along the orbit, any fluid capable of motion relative to the spacecraft is subject to the acceleration that arises from the gravity gradients of the Earth.[8–10] The interaction between the particle mass of fluid and the spacecraft mass due to gravity-gradient acceleration[9] can excite slosh waves. In this study, comparisons are made for the dynamical evolution of slosh-waves excited by driving forces due to gravity-gradient acceleration.

In order to reduce the asymmetry in liquid-vapor distribution that is induced by slosh waves excited by asymmetric gravity-gradient acceleration, a number of baffle boards are installed inside the Dewar (as shown in Fig. 1). Comparison will be made between the degrees of asymmetry in liquid-vapor distribution in a Dewar with and without a baffles during slosh-wave excitation induced by asymmetric gravity-gradient acceleration acting on the spacecraft. In this study, we investigate the time evolution of the profile of the liquid-vapor interface and the center-of-mass fluctuations for a rotating Dewar container with and without a baffle boards.

Model of Slosh-Wave Excitation at the Interface

Consider a closed circular Dewar that is partially filled with liquid helium, the ullage being filled with helium vapor. A noninertial frame of spacecraft-bound coordinates is adopted in the mathematical formulation. In this formulation, the Coriolis force $(2\rho\omega v, -2\rho\omega u, 0)$, centrifugal force $(\rho r\omega^2, 0, 0)$, angular acceleration $(0, \rho r\dot{\omega}, 0)$, and gravity-gradient acceleration $(a_{gg,r}, a_{gg,\theta}, a_{gg,z})$ along the cylindrical coordinate (r, θ, z) for a rotating Dewar with angular velocity $(0, 0, \omega)$ are considered. The governing equations are as follows:

1) continuity equation:

$$\frac{1}{r}\frac{\partial}{\partial r}(ru) + \frac{1}{r}\frac{\partial v}{\partial \theta} + \frac{\partial w}{\partial z} = 0 \tag{1}$$

2) momentum equations:

$$\rho\left(\frac{\partial u}{\partial t} + u\frac{\partial u}{\partial r} + \frac{v}{r}\frac{\partial u}{\partial \theta} - \frac{v^2}{r} + w\frac{\partial u}{\partial z}\right)$$
$$= -\frac{\partial p}{\partial r} + 2\rho\omega v + \rho(a_{gg,r}) + \rho r\omega^2$$
$$+ \mu\left(\nabla^2 u - \frac{u}{r^2} - \frac{2}{r^2}\frac{\partial v}{\partial \theta}\right) \tag{2}$$

$$\rho\left(\frac{\partial v}{\partial t} + u\frac{\partial v}{\partial r} + \frac{v}{r}\frac{\partial v}{\partial \theta} + \frac{uv}{r} + w\frac{\partial v}{\partial z}\right)$$
$$= -\frac{1}{r}\frac{\partial p}{\partial \theta} - 2\rho\omega u + \rho(a_{gg,\theta}) + \rho r\dot{\omega}$$
$$+ \mu\left(\nabla^2 v - \frac{v}{r^2} + \frac{2}{r^2}\frac{\partial u}{\partial \theta}\right) \tag{3}$$

$$\rho\left(\frac{\partial w}{\partial t} + u\frac{\partial w}{\partial r} + \frac{v}{r}\frac{\partial w}{\partial \theta} + w\frac{\partial w}{\partial z}\right)$$
$$= -\frac{\partial p}{\partial z} + \rho(a_{gg,z}) + \mu\nabla^2 w \tag{4}$$

where

$$\nabla^2 = \frac{1}{r}\frac{\partial}{\partial r}\left(r\frac{\partial}{\partial r}\right) + \frac{1}{r^2}\frac{\partial^2}{\partial \theta^2} + \frac{\partial^2}{\partial z^2} \tag{5}$$

In the computation of the fluid forces, moment, viscous stress, and angular momentum acting on the container wall of the spacecraft, one has to consider the velocity in an inertial frame rather than relative to the rotating coordinates in the noninertial frame. In other words, one has to substitute

$$v = v' - r\omega \tag{6}$$

into the governing equations for the purpose of computing forces acting on the container of the rotating system. Here v' is the absolute circumferential velocity in the rotating system, and v is the relative circumferential velocity.

For the purpose of solving dynamical problems of sloshing liquid propellant systems in orbital spacecraft in a microgravity environment, one has to solve the governing equations shown in Eqs. (1–5) subject to a set of initial and boundary conditions. A precise and detailed exposition of these initial and boundary conditions has been given by Hung and Pan.[11] A computational algorithm applicable to cryogenic-fluid management under microgravity was also given in our earlier studies.[3–5] In this study, to show a realistic example, a full-scale model of the GP-B spacecraft propellant Dewar tank with an outer radius of 68 cm, an inner radius of 13 cm, top and bottom dome radii of 80 cm, and a height of 145 cm was used in the numerical simulation. The propellant tank is 80% filled with liquid helium, and the ullage is filled with helium vapor. The temperature of the helium is 1.8 K. In this study the following data were used: liquid-helium density = 0.146 g/cm^3, helium vapor density = 0.00147 g/cm^3, fluid pressure = 1.66×10^4 dyne/cm^2, surface-tension coefficient at the interface between liquid helium and helium vapor = 0.353 dyne/cm, liquid-helium viscosity coefficient = 9.61×10^{-5} cm^2/s, and contact angle = 5 deg. The initial profiles of the liquid-vapor interface for the rotating Dewar are determined from computations based on algorithms developed for the steady-state formulation of microgravity fluid management.[3–5]

A staggered grid for the velocity components is used in this computer program. The method was developed by Harlow and Welch[12] for their marker-and-cell (MAC) method of studying fluid flows along a free surface. The finite-difference method employed in this numerical study was the "hybrid scheme" developed by Spalding.[13] The formulation for this method is valid for any arbitrary interface location between the grid points and is not limited to midpoint

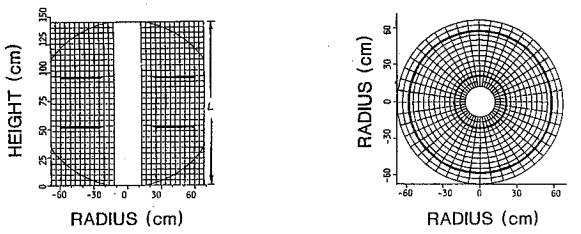

Fig. 2 Distribution of grid points in a) the radial-axial plane and b) the radial-circumferential plane of the cylindrical coordinates for GP-B Dewar tank.

interfaces.[14] An algorithm for a semi-implicit method[15] was used as the procedure for modeling the flowfield. The time step is determined automatically from the spacing of the grid points and the velocity of the flowfields. More than 200 iterations were applied for each time step to assure the convergence of the series. To conserve the volume of liquid, a deviation of less than 1% in volume is required before a move to the next time step. A detailed description of the computational algorithm applicable to microgravity fluid management is illustrated in our earlier studies.[3–5] The results of our steady-state computations have been compared with the experimental observations made by Leslie[6] in a free-falling aircraft (KC-135), yielding excellent agreement. Time-dependent experimental results on sloshing dynamics in a microgravity environment are not available for comparison at this time, but will be obtained by NASA Goddard Space Flight Center during shuttle experiments in the near future to verify the model computation. Figures 2a and 2b show the distribution of grid points for the Dewar tank in the radial-axial plane and radial-circumferential plane, respectively, in cylindrical coordinates.

Interface Disturbances Driven by Gravity-Gradient Acceleration

For the case of the GP-B spacecraft, which is an Earth satellite orbiting at 650-km altitude directly over the poles, the orbit period τ_0 can be computed from the following expression[1,9]:

$$\tau_0 = 2\pi \frac{R_C^{\frac{3}{2}}}{R_E g_0^{\frac{1}{2}}} \tag{7}$$

For GP-B, the orbit period $\tau_0 = 97.6$ min, and the orbit rate $n = 2\pi/\tau_0 = 1.07 \times 10^{-3}$ rad/s.

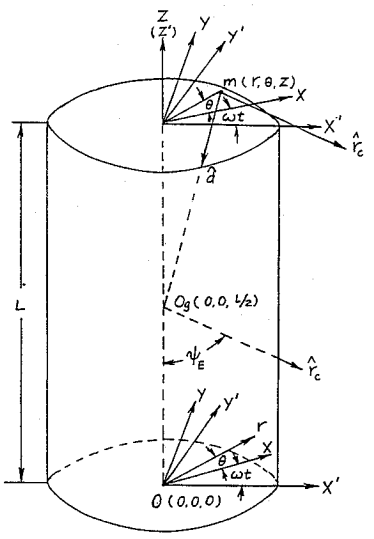

Fig. 3 Coordinate systems for the computation of gravity-gradient acceleration: (x', y', z') in inertial coordinate system, and (x, y, z) in noninertial, spacecraft-bound coordinate system.

The gravity-gradient acceleration acting on the fluid mass in the spacecraft can be shown to be[9,10,16]

$$\hat{a}_{gg} = -n^2[3(\hat{r}_c \cdot \hat{d})\hat{f}_c - \hat{d}] \tag{8}$$

For the case of the GP-B spacecraft, it is assumed that the gravity gradient exerted on the mass center of the spacecraft orbiting around the Earth on its specified orbit is zero. In other words, the entire gravity acceleration exerted on the spacecraft consists of the gravity-gradient acceleration defined in Eq. (8). In this study, we are interested in investigating how gravity-gradient acceleration affects the dynamical behavior of the fluid elements of the helium.

For convenience of calculation, let us describe all the parameters involved in Eq. (8) in terms of Cartesian coordinates. In order to match the computer simulation, mathematical derivations are considered in the first quadrant. Figure 3 illustrates the geometrical relationship of the parameters shown in Eq. (8).

The gravity-gradient acceleration acting on the fluid element located at (r, θ, z) can be transformed to the cylindrical, noninertial coordinates as follows[16]:

$$\hat{a}_{gg} = \begin{bmatrix} a_{gg,r} \\ a_{gg,\theta} \\ a_{gg,z} \end{bmatrix} = -n^2 \begin{bmatrix} \cos(\theta+\omega t) & \sin(\theta+\omega t) & 0 \\ -\sin(\theta+\omega t) & \cos(\theta+\omega t) & 0 \\ 0 & 0 & 1 \end{bmatrix} \begin{bmatrix} 3[(z-L/2)\cos\Psi_E - r\cos(\theta+\omega t)\sin\Psi_E]\sin\Psi_E + r\cos(\theta+\omega t) \\ r\sin(\theta+\omega t) \\ -3[(z-L/2)\cos\Psi_E - r\cos(\theta+\omega t)\sin\Psi_E]\cos\Psi_E + (z-L/2) \end{bmatrix} \tag{9}$$

At time $t = 0$, the rotational axis of the spacecraft is aligned with the radial direction from the Earth center to the spacecraft mass center. Assuming that the spacecraft axis of rotation is turns linearly from 0 to 360 deg in 600 s while the spacecraft is orbiting around the Earth, the azimuth angle ψ_E can be defined as

$$\psi_E = 2\frac{\pi}{\tau}t \tag{10}$$

Here, t is the time measured from the instant when the direction of the spacecraft axis of rotation is aligned with the radial direction from the spacecraft mass center to the center of the Earth.

Interface Oscillations without a Baffle Board

The equilibrium shape of the liquid-vapor interface for a rotating Dewar without a baffle boards, with a background gravity environment of 10^{-7} g_0 and a rotation speed of 0.1 rpm, is a doughnut configuration with a near-circular, kidney-shaped cross section, according to a computation with the numerical algorithm developed in our earlier studies.[3–5] The top part of Fig. 4 shows, from left to right, the initial profile of the three-dimensional liquid-vapor interface; initial shape of the interface in the r-z plane at $\theta = 0$ and 180 deg, and the same at $\theta = 90$ and 270 deg. In this paper, we shall confine ourselves to the time evolution of interface oscillations due to sloshing dynamic disturbances driven by gravity-gradient acceleration in the r-z plane at $\theta = 0$ and 180 deg only, as well as the three-dimensional profile.

Figure 5 shows the time evolution of the three-dimensional dynamical behavior of the liquid-vapor interface oscillations driven by gravity-gradient acceleration acting on a rotating Dewar without a baffle boards. For convenience of comparison, liquid-vapor interface profiles with the same time values were calculated for this paper. The six values of time chosen throughout this paper are $t = 60$, 150, 240, 450, 510, and 600 s. The results clearly show that there is a series of asymmetric sloshing oscillations excited along the liquid-vapor interface, driven by asymmetric gravity-gradient acceleration.

Careful examination of the gravity-gradient equations shown in Eq. (9) indicates that there are greater positive components of acceleration longitudinal to the direction from the spacecraft mass center

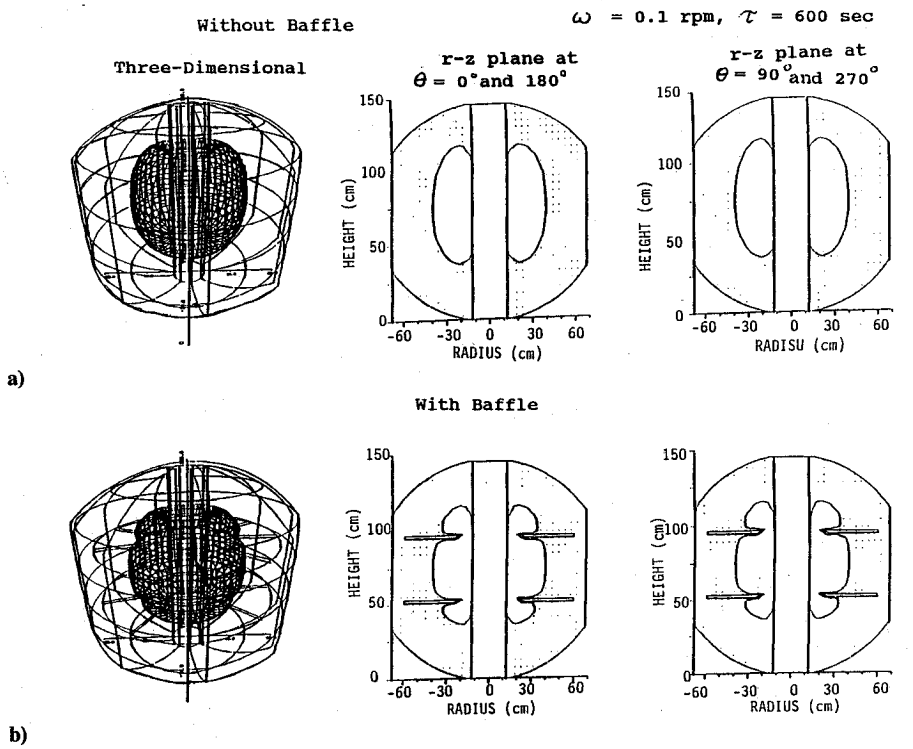

Fig. 4 Initial profiles of liquid-vapor interface for GP-B module of rotating Dewar without and with baffles.

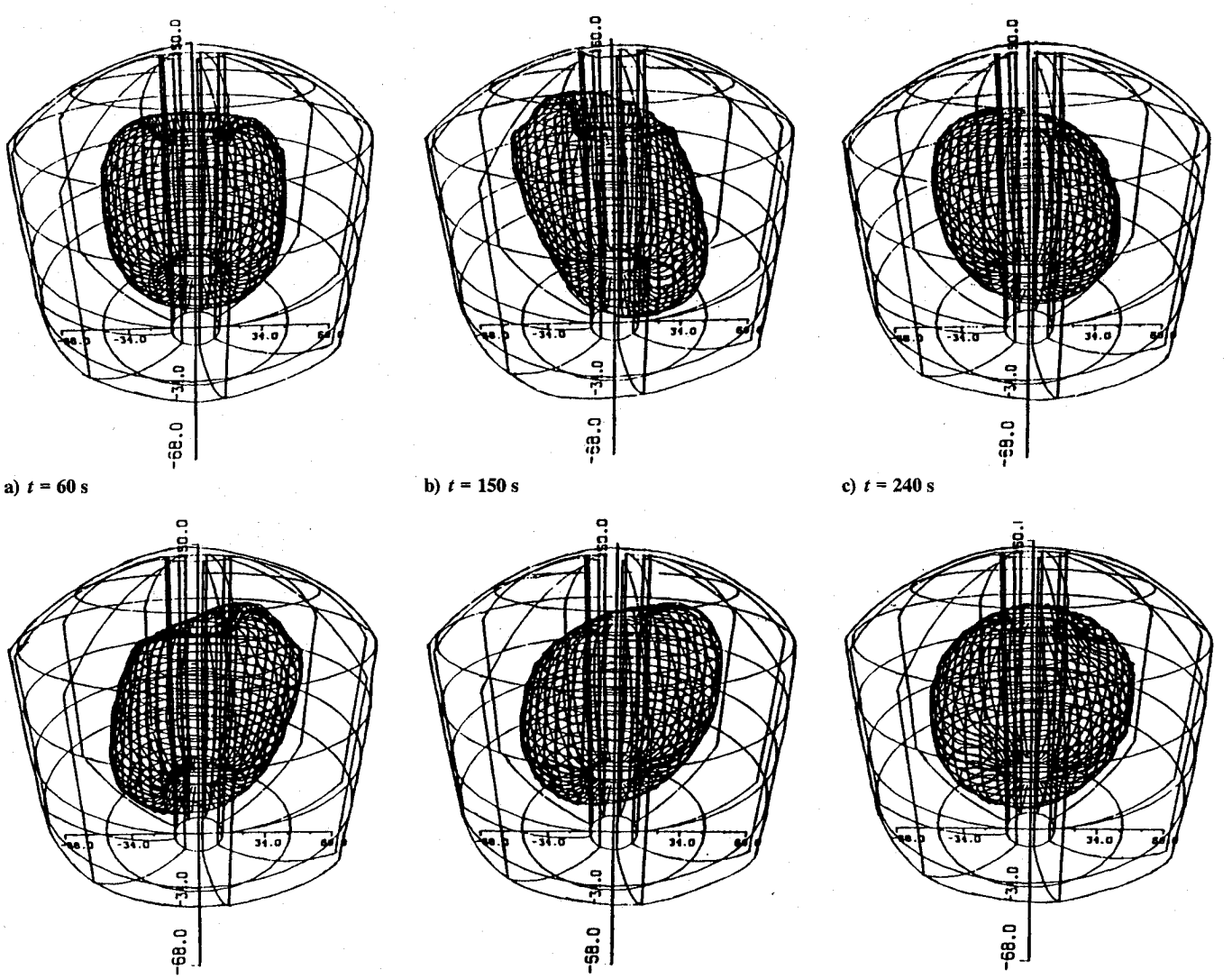

Fig. 5 Time evolution of three-dimensional liquid-vapor interface oscillations without baffles.

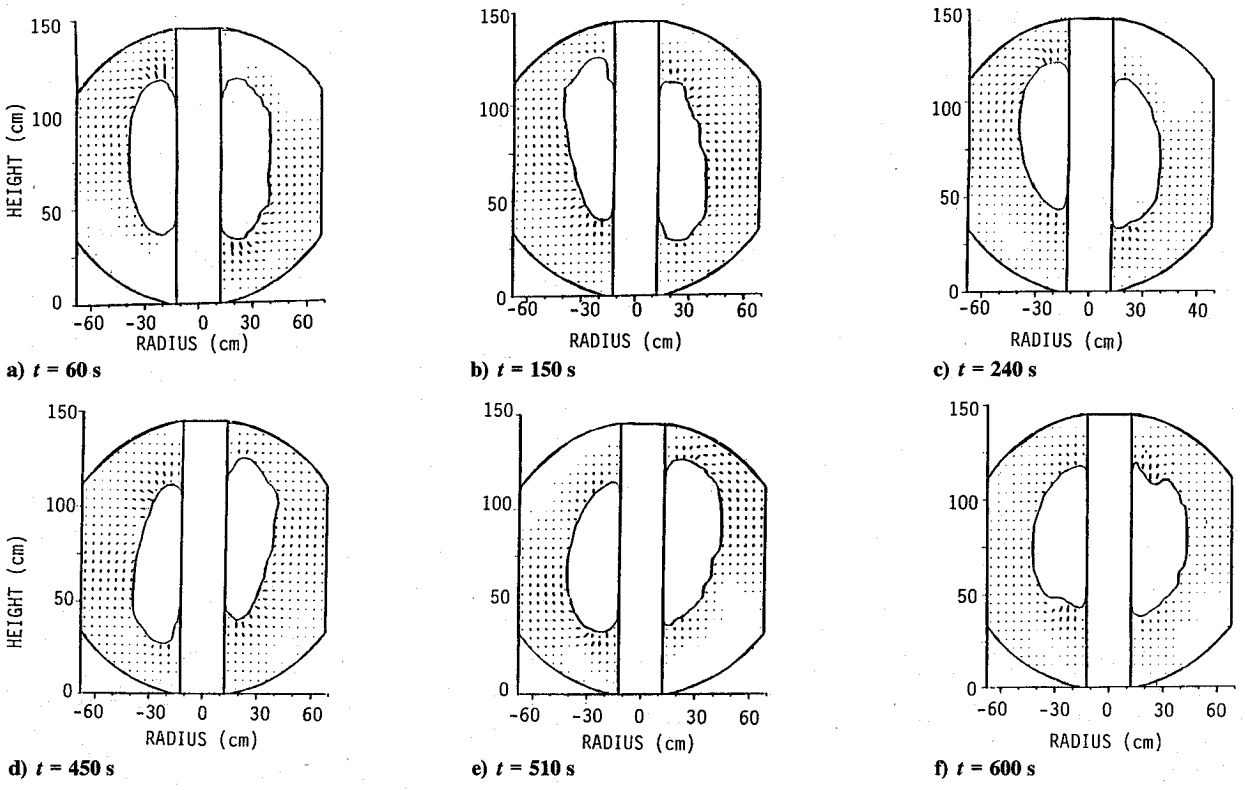

Fig. 6 Time evolution of liquid-vapor interface oscillations without baffles for rotating Dewar in r-z plane at $\theta = 0$ and 180 deg.

to the Earth center, and smaller negative components of acceleration transverse to this direction. As we indicated in Eq. (10), the angle ψ_E varies with time. This phenomenon shows that the gravity-gradient acceleration exerted on the spacecraft is equivalent to the combination of a time-dependent force in the turnaround direction and a torsional moment acting on the spacecraft when it is orbiting around the Earth. It is seen in Fig. 5 that the deformation of the bubble is created by an asymmetric torsional moment with a twisting force.

The evolution of the interface oscillations at various cross sections is also examined. For example, Fig. 6 shows the time sequence of the liquid-vapor interface profiles, driven by the same gravity-gradient acceleration as that shown in Fig. 5, in the vertical r-z plane at $\theta = 0$ and 180 deg. It indicates that the doughnut-shaped bubble (helium vapor) changes from axially symmetric to asymmetric profiles in a plane aligned with the vector of gravity-gradient acceleration, and the axis of rotation as ψ_E varies from 0 to 360 deg.

The one-up one-down and one-down one-up oscillations of two bubbles in the cross section of doughnut profiles in the vertical r-z plane, shown in Fig. 6, indicate a very important characteristic of gravity-gradient acceleration, which produce a combination of time-dependent equivalent torsional moment and twisting force acted on the spacecraft when it is orbiting around the Earth.

Interface Oscillations with Baffles Installed

For the purpose of reducing the degree of asymmetry in the liquid-vapor distribution, two baffle boards were installed in the Dewar, with an inner radius of 20.87 cm, an outer radius of 59.43 cm, and a thickness of 1.93 cm. These two baffles are located at $z_1 = 53.16$ cm and $z_2 = 96.67$ cm. The rest of the conditions are similar to the Dewar without baffle boards, discussed earlier. The bottom part of Figures 4 shows, from left to right, the initial shape of the three-dimensional interface profile, the interface in the r-z plane at $\theta = 0$ and 180 deg, and the same at $\theta = 90$ and 270 deg, for a rotating Dewar with baffle boards. As in the previous cases for bubble oscillations without baffles, we shall confined ourselves here to the time evolution in three-dimensional profiles and in the r-z plane at $\theta = 0$ and 180 deg.

Figure 7 shows the time evolution of the three-dimensional dynamical behavior of the liquid-vapor interface oscillations driven by gravity-gradient acceleration acting on a rotating Dewar with baffle boards. Comparison between Figs. 5 and 7 shows a greater degree of asymmetry in the excitation of slosh-waves along the liquid-vapor interface without baffles than with baffles.

We have also examined the time evolution of the three-dimensional profiles of the liquid-vapor interface oscillations at various cross sections, driven by the same gravity-gradient acceleration acting on a rotating Dewar with baffle boards. For example, Fig. 8 shows the time evolution of the dynamical behavior of the liquid-vapor interface profiles, driven by the same gravity-gradient acceleration as that shown in Fig. 5, in the vertical r-z plane at $\theta = 0$ and 180 deg, for a rotating Dewar with baffles. Like Fig. 6, Fig. 8 also shows that the doughnut-shaped bubble (helium vapor) configurations change from axially symmetric to asymmetric profiles in a plane aligned with the direction of background gravity and with the axis of rotation as ψ_E varies from 0 to 360 deg for a rotating Dewar with baffles installed. Comparison of Figs. 6 and 8 shows a greater degree of asymmetry for the excitation of slosh waves without baffles than with baffles.

Again, the one-up one-down and one-down one-up oscillations of two bubbles, partially cut by baffle boards, in the cross section of doughnut profiles in the vertical r-z plane, shown in Fig. 8 with baffles installed, indicate a very important characteristic of gravity-gradient acceleration, which produces a combination of time-dependent equivalent torsional moment and twisting force acting on the spacecraft when it is orbiting around the Earth.

Time Evolution of Bubble Mass-Center Fluctuations

With the conditions shown earlier, one can compute the time evolution of the locations of bubble mass-center fluctuations for a rotating Dewar with and without baffles, based on the information on time-dependent fluctuations of the liquid-vapor interface shown in Figs. 4 (top), 5, and 6 and in Figs. 4 (bottom), 7, and 8, respectively.

Figures 9a and 9b show the time fluctuations of the locations of bubble mass centers in the rotating Dewar without and with baffle

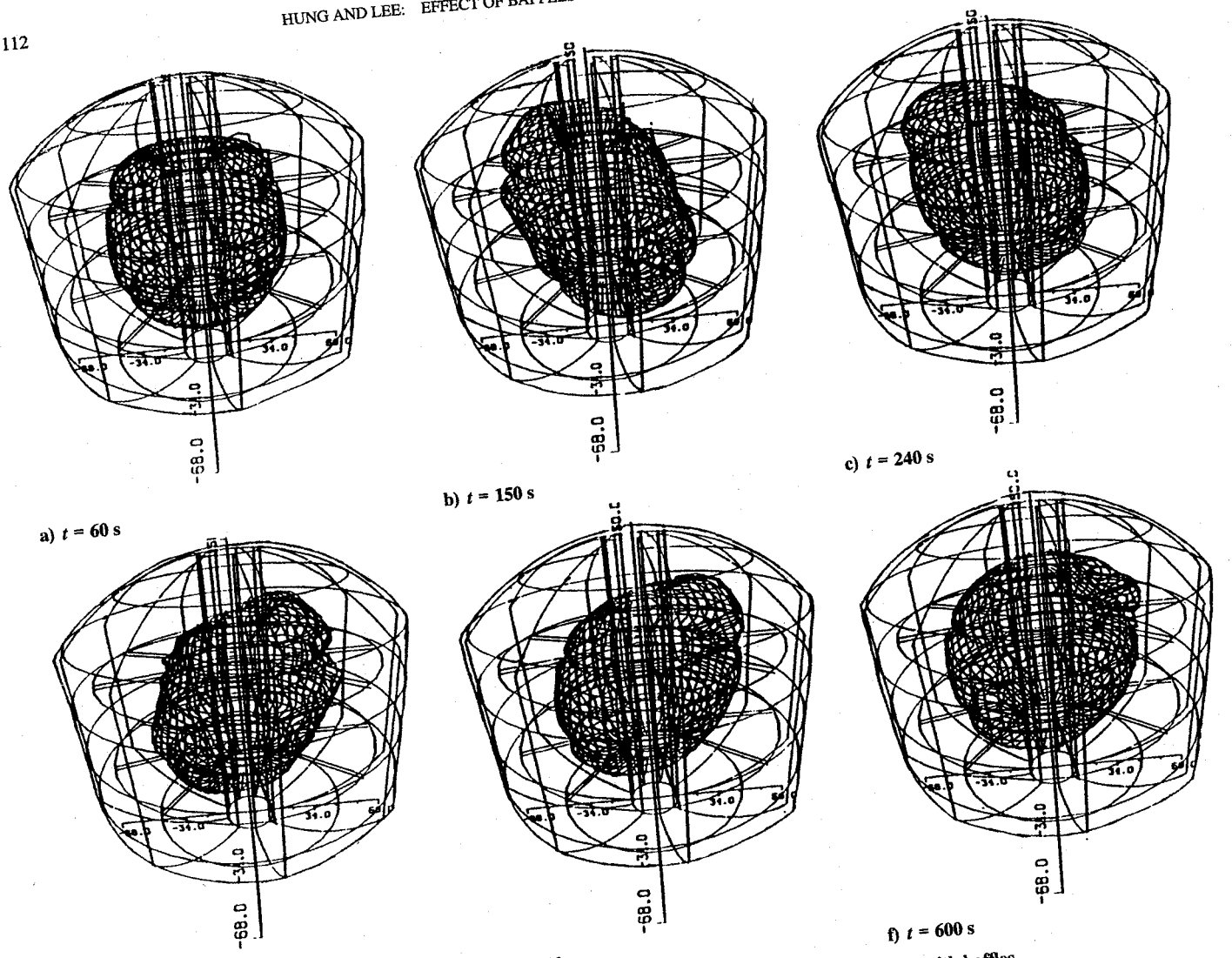

a) t = 60 s b) t = 150 s c) t = 240 s

d) t = 450 s e) t = 510 s f) t = 600 s

Fig. 7 Time evolution of three-dimensional liquid-vapor interface oscillations with baffles.

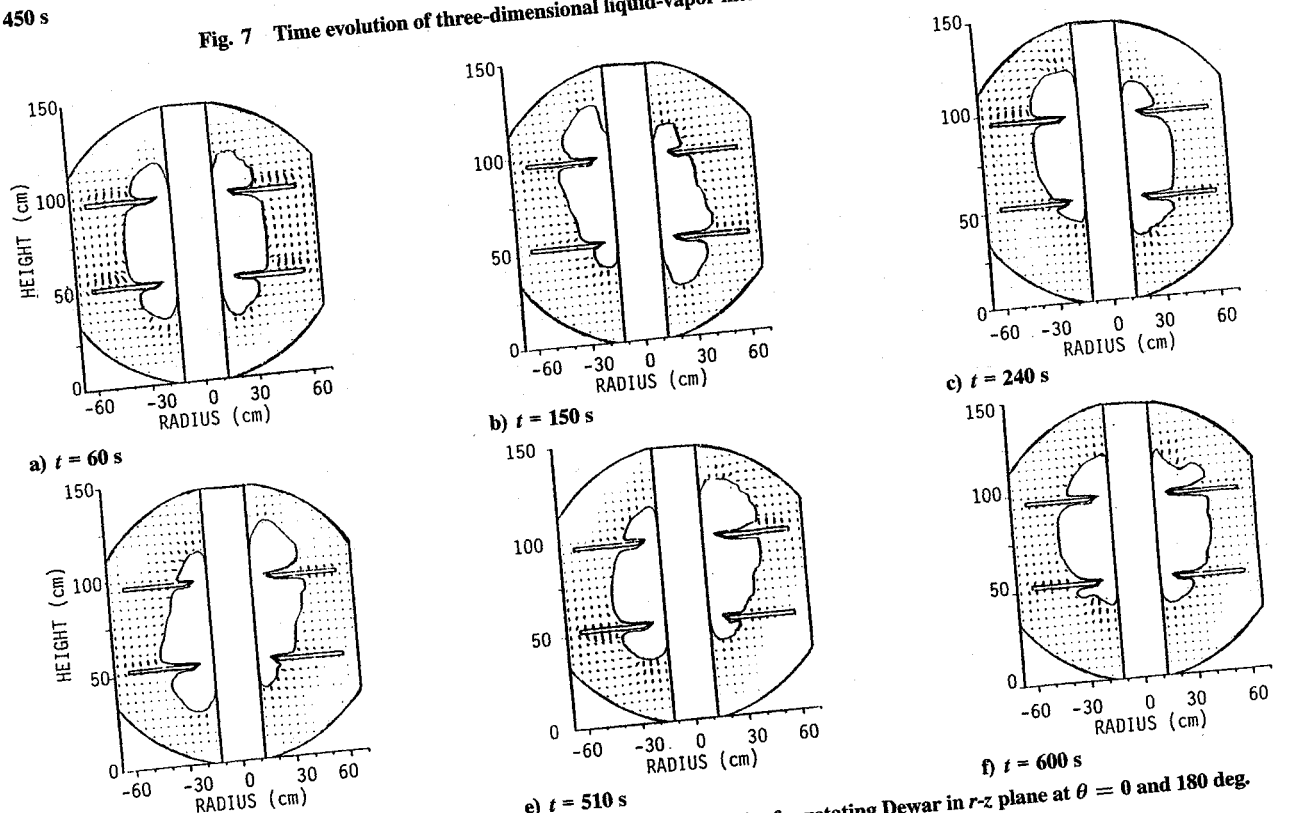

a) t = 60 s b) t = 150 s c) t = 240 s

d) t = 450 s e) t = 510 s f) t = 600 s

Fig. 8 Time evolution of liquid-vapor interface oscillations with baffles for rotating Dewar in r-z plane at $\theta = 0$ and 180 deg.

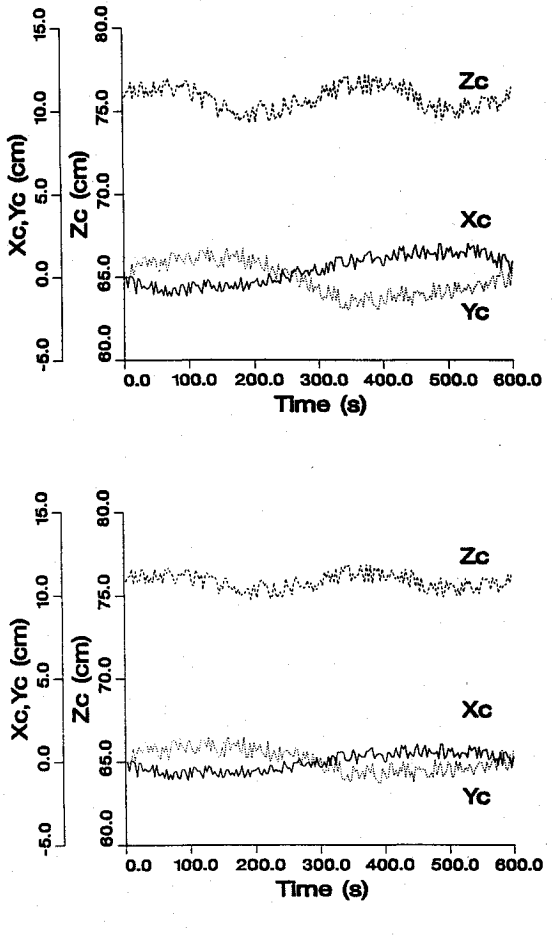

Fig. 9 Time sequences of bubble mass-center fluctuations caused by slosh-wave excitation driven by gravity-gradient acceleration in rotating Dewar: a) without baffles and b) with baffles.

boards, respectively. The curves of x_c (solid line), y_c (dotted line), and z_c (broken line) represent the time dependence of the location of the bubble mass center along the x, y, and z axes, respectively.

The magnitudes of the bubble mass-center fluctuations for the rotating Dewar without baffles are $(\Delta x_c, \Delta y_c, \Delta z_c) = (3.2, 3.7, 3.0)$ cm, and with baffles are $(\Delta x_c, \Delta y_c, \Delta z_c) = (2.2, 2.8, 2.1)$ cm. Comparison between Figs. 9a and 9b leads to the following conclusions:

1) The torsional moment and twisting force due to gravity-gradient acceleration exerted on the rotating Dewar container produce greater fluctuations without baffles than with baffles.

2) The dynamics of the bubble (liquid-vapor interface) driven by the torsional moment and twisting force produce bubble mass-center fluctuations with magnitudes $\Delta y_c > \Delta x_c > \Delta z_c$.

3) Comparison of the bubble mass-center fluctuations without and with baffles shows that they are greater without baffles.

4) The fluctuations of both x_c and y_c start from zero, while that of z_c starts from a nonzero value at the mid point of the height of the partially filled container.

Discussion and Conclusion

The dynamical behavior of cryogenic-liquid propellant affected by asymmetric gravity-gradient acceleration has been studied. An example applicable to the GP-B spacecraft Dewar with and without baffle boards has been given a treatment by numerically solving the three-dimensional Navier-Stokes equations subject to the initial and boundary conditions. The initial conditions for the liquid-vapor interface profiles were adopted from the steady-state formulation of the rotating Dewar developed by Hung et al.[3,17]

In this study, the spacecraft gravity turnaround time is assumed to be 600 s, which is the same as the period of the spacecraft rotation. Results on slosh-wave excitation along the liquid-vapor interface induced by gravity-gradient acceleration indicated that the gravity-gradient acceleration exerted on the spacecraft is equivalent to the combination of a time-dependent twisting force in the turnaround direction and a torsional moment acting on the spacecraft when it is orbiting around the Earth. The action of these forces and moments induces one-up one-down and one-down one-up oscillations of two bubbles with doughnut profiles in the vertical r-z plane of the rotating Dewar. The equivalent twisting force and torsional moment also induce an eccentric contour of the bubble's horizontal cross section in the r-θ plane, which oscillates and rotates clockwise.

The viscous force between liquid and solid greatly contributes to the damping effect of slosh-wave excitation, and a rotating Dewar with baffles provides more area of liquid-solid interface than one without baffles.[18] The three-dimensional simulation of the time evolution of liquid-vapor interface oscillations driven by the asymmetric gravity-gradient disturbances shows that the greater damping provided by the baffle reduces the amplitude of slosh-wave excitation, which, in turn, reduces the asymmetry in the liquid-vapor interface. Computation of the time-dependent bubble mass-center fluctuations also verifies that a rotating Dewar with baffles produces less fluctuation than one without baffles.

Time-variations in the directions of the gravity-gradient acceleration imposed on the spacecraft will change the asymmetry distribution of the liquid-vapor interface in the rotating Dewar container. This means that both the moment of inertia and the angular momentum of the spacecraft will be greatly affected by the presence of asymmetric fluctuations in the liquid-vapor interface.[17–19] In this study, it is shown that the installation of baffles can provide greater damping to reduce the development of large-amplitude slosh waves along the liquid-vapor interface. These results will be useful for the handling and managing the cryogenic-liquid propellant to be used in the spacecraft propulsion system.[17,18]

Acknowledgments

The authors appreciate the support received from the National Aeronautics and Space Administration through the NASA Grant NAG8-938 and NAS8 Contract NAS8-38609, Deliver Order 103. They would like to express their gratitude to Richard A. Potter of NASA/Marshall Space Flight Center for the stimulating discussions during the course for the present study.

References

[1]Wilkinson, D. T., Bender, P. L., Eardley, D. M., Gaisser, T. K., Hartle, J. B., Israel, M. H., Jones, L. W., Partridge, R. B., Schramm, D. N., Shapiro, I. I., Vessort, R. F. C., and Wagoner, R. V., "Gravitation, Cosmology and Cosmic-Ray Physics," *Physics Today*, Vol. 39, 1986, pp. 43–46.

[2]Kamotani, Y., Prasad, A., and Ostrach, S., "Thermal Convection in an Enclosure Due to Vibrations aboard a Spacecraft," *AIAA Journal*, Vol. 19, 1981, pp. 511–516.

[3]Hung, R. J., Lee, C. C., and Leslie, F. W., "Response of Gravity Level Fluctuations on the Gravity Probe-B Spacecraft Propellant System," *Journal of Propulsion and Power*, Vol. 7, 1991, pp. 556–564.

[4]Hung, R. J., and Shyu, K. L., "Space-Based Cryogenic Liquid Hydrogen Reorientation Activated by Low Frequency Impulsive Reverse Thruster of Geyser Initiation," *Acta Astronautica*, Vol. 25, 1991, pp. 709–719.

[5]Hung, R. J., and Shyu, K. L., "Constant Reverse Thrust Activated Reorientation of Liquid Hydrogen with Geyser Initiation," *Journal of Spacecraft and Rockets*, Vol. 29, 1992, pp. 279–285.

[6]Leslie, F. W., "Measurements of Rotating Bubble Shapes in a Low Gravity Environment," *Journal of Fluid Mechanics*, Vol. 161, 1985, pp. 269–279.

[7]Mason, P., Collins, D., Petrac, D., Yang, L., Edeskuty, F., Schuch, A., and Williamson, K., "The Behavior of Superfluid Helium in Zero Gravity," *Proceedings of the 7th International Cryogenic Engineering Conferences*, Surrey, England, Science and Technology Press, 1978.

[8]Avduyevsky, V. S. (ed.), *Scientific Foundations of Space Manufacturing*, MIR, Moscow, 1984.

[9]Forward, R. L., "Flattening Space-Time Near the Earth," *Physical Review A*, Vol. 26, 1982, pp. 735–744.

[10]Misner, C. W., Thorne, K. S., and Wheeler, J. A., *Gravitation*, W. H. Freeman, San Francisco, 1973, pp. 1–1279.

[11]Hung, R. J., and Pan, H. L., "Asymmetric Slosh-Wave Excitation in Liquid-Vapor Interface under Microgravity," *Acta Mechanica Sinica*, Vol. 9, 1993, pp. 298–311.

[12]Harlow, F. H., and Welch, F. E., "Numerical Calculation of Time-Dependent Viscous Incompressible Flow of Fluid with Free Surface," *Physics of Fluids*, Vol. 8, 1965, pp. 2182–2189.

[13]Spalding, D. B., "A Novel Finite-Difference Formulation for Differential Expressions Involving Both First and Second Derivatives," *International Journal of Numerical Methods in Engineering*, Vol. 4, 1972, pp. 551–559.

[14]Patanker, S. V., *Numerical Heat Transfer and Fluid Flow*, Hemisphere-McGraw-Hill, New York, 1980, p. 197.

[15]Patanker, S. V., and Spalding, S. D., "A Calculation Procedure for Heat, Mass and Momentum Transfer in Three Dimensional Parabolic Flows," *International Journal of Heat and Mass Transfer*, Vol. 15, 1972, pp. 1787–1805.

[16]Hung, R. J., Pan, H. L., and Leslie, F. W., "Gravity-Gradient or Gravity Jitter Induced Viscous Stress and Moment Fluctuations in Microgravity," *Fluid Dynamics Research*, Vol. 14, 1994, pp. 29–51.

[17]Hung, R. J., Lee, C. C., and Leslie, F. W., "Spacecraft Dynamical Distribution of Fluid Stresses Activated by Gravity Jitter Induced Slosh Waves," *Journal of Guidance, Control and Dynamics*, Vol. 15, 1992, pp. 817–824.

[18]Hung, R. J., Lee, C. C., and Leslie, F. W., "Effect of the Baffle on the Spacecraft Fluid Propellant Viscous Stress and Moment Fluctuations," *Transactions of the Japan Society for Aeronautical and Space Sciences*, Vol. 35, 1993, pp. 187–207.

[19]Hung, R. J., Lee, C. C., and Leslie, F. W., "Similarity Rules in Gravity Jitter-Related Spacecraft Liquid Propellant Slosh-Wave Excitation," *Journal of Fluids and Structures*, Vol. 6, 1992, pp. 493–522.